Science Translational Medicine
AAAS

www.sciencetranslationalmedicine.org/cgi/content/full/10/468/eaat6420/DC1

Supplementary Materials for

Two recombinant human monoclonal antibodies that protect against lethal Andes hantavirus infection in vivo

Jose L. Garrido, Joseph Prescott, Mario Calvo, Felipe Bravo, Raymond Alvarez, Alexis Salas, Raul Riquelme, Maria L. Rioseco, Brandi N. Williamson, Elaine Haddock, Heinz Feldmann, Maria I. Barria*

*Corresponding author. Email: mbarriac@udec.cl

Published 21 November 2018, *Sci. Transl. Med.* **10**, eaat6420 (2018)
DOI: 10.1126/scitranslmed.aat6420

The PDF file includes:

Other Supplementary Material for this manuscript includes the following:

(available at www.sciencetranslationalmedicine.org/cgi/content/full/10/468/eaat6420/DC1)

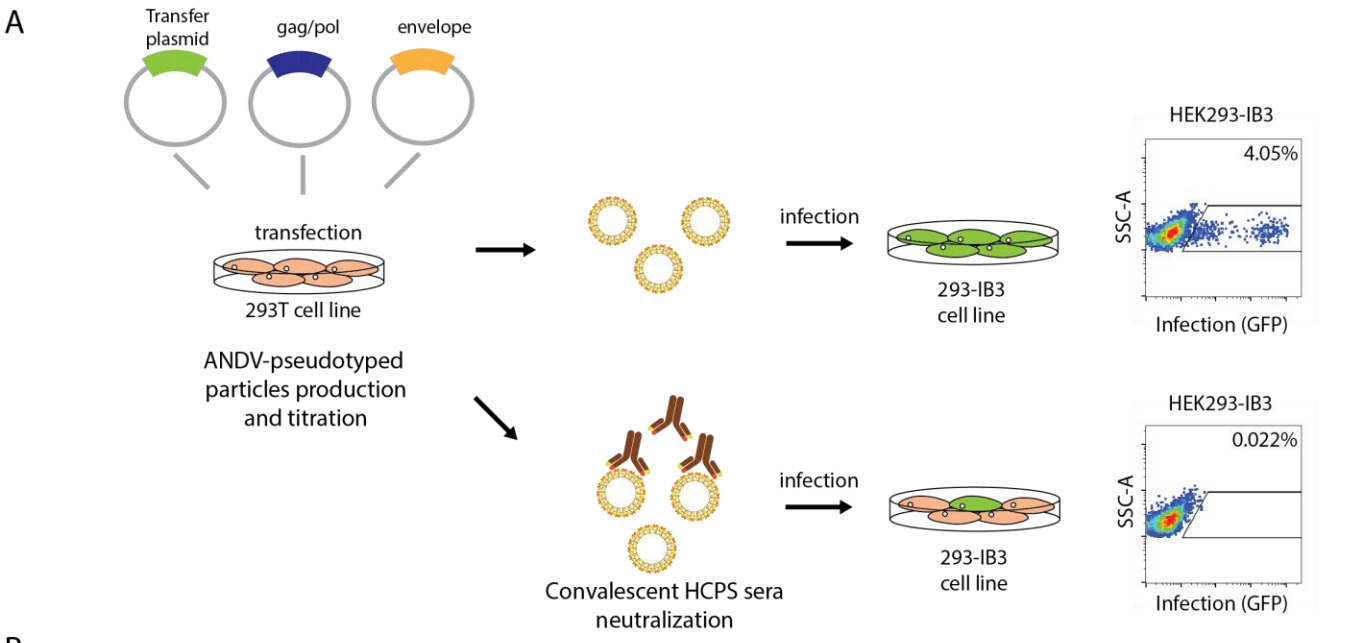
A
Transfer plasmid
gag/pol
envelope
transfection
293T cell line
ANDV-pseudotyped particles production and titration
infection
293-IB3 cell line
HEK293-IB3
4.05%
SSC-A
Infection (GFP)
Convalescent HCPS sera neutralization
infection
293-IB3 cell line
HEK293-IB3
0.022%
SSC-A
Infection (GFP)

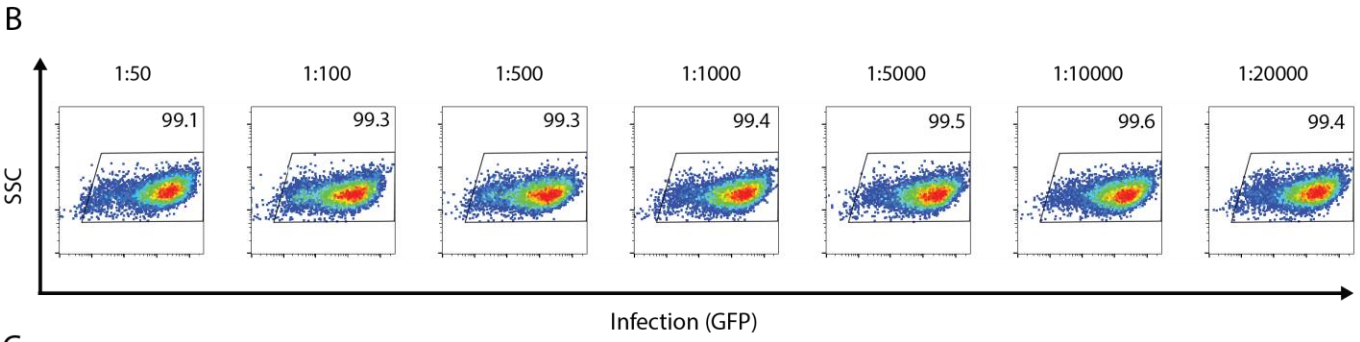
B
1:50
1:100
1:500
1:1000
1:5000
1:10000
1:20000
99.1
99.3
99.3
99.4
99.5
99.6
99.4
SSC
Infection (GFP)

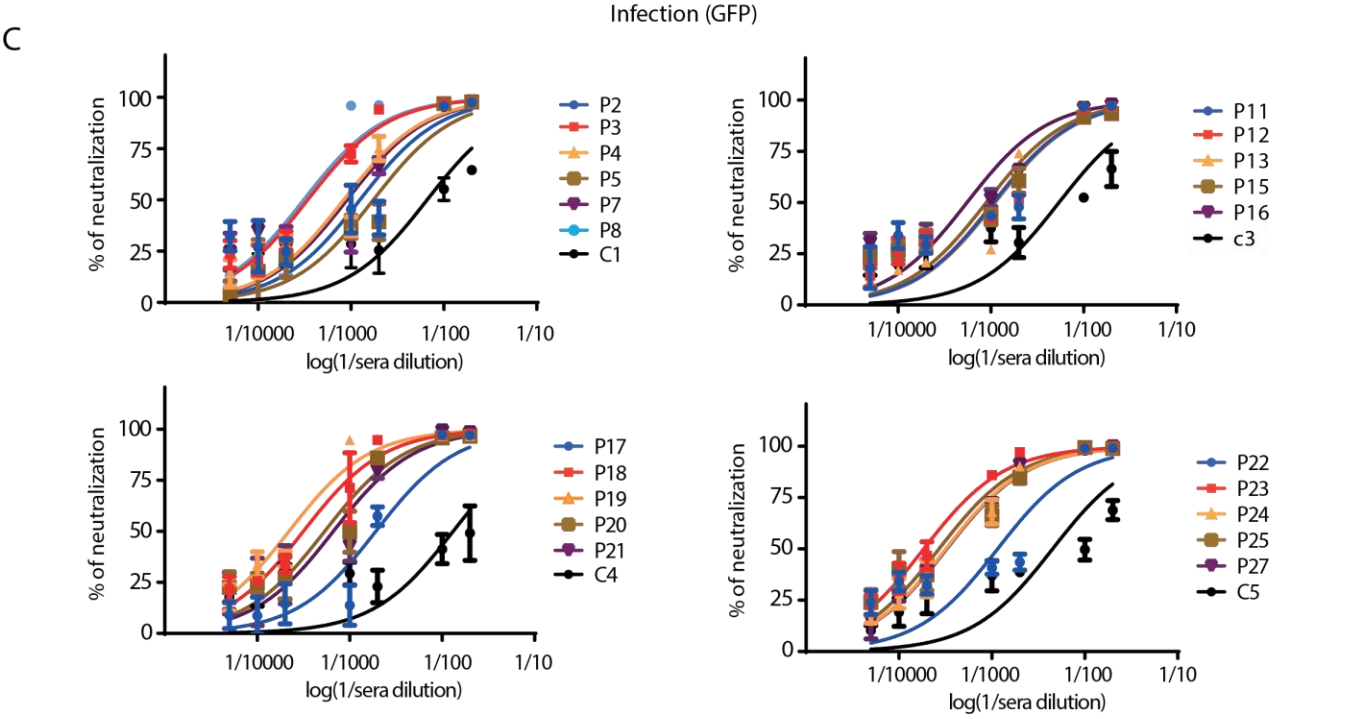
C
% of neutralization
log(1/sera dilution)
1/10000
1/1000
1/100
1/10
P2
P3
P4
P5
P7
P8
C1
P11
P12
P13
P15
P16
c3
P17
P18
P19
P20
P21
C4
P22
P23
P24
P25
P27
C5

Fig. S1. Neutralization assay. (A) HEK293 cells stably transduced with β3 integrin (HEK293-IB3) were used as target cells for ANDV infection. ANDV pseudotyped particles (ANDV-pv) were incubated with different dilutions of sera from ANDV convalescent or healthy subjects and the frequency of infected cells analyzed by flow cytometry. Upon productive infection, is produce green fluorescent protein (GFP). A representative dot plot is shown. **(B)** As a nonspecific control of sera inhibition, VSV-G-pv were used to infect target cells in the presence of convalescent sera. VSV-G-pv were incubated with sera from ANDV convalescent subjects at different dilutions (1:50-1:20,000) and used to infect HEK293-IB3 cells. Representative dot plots are shown. **(C)** Neutralization curves of the ANDV convalescent (P2-P27) and healthy controls (C1-C5) sera, the y-axis displays the percentage of pseudovirus neutralization and the x-axis the reciprocal of the dilution in log.

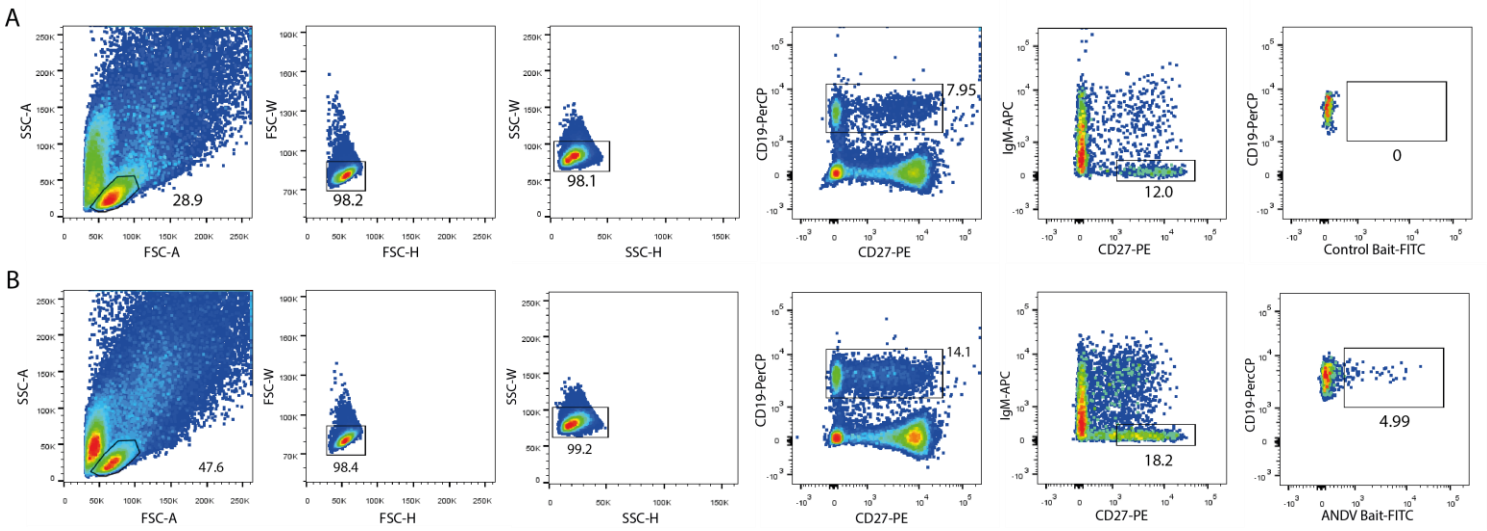

Fig. S2. Single-cell sorting gating strategy. PBMCs from convalescent subject P10 were stained using anti-human Abs: anti-CD19-PerCP-Vio700, anti-CD27-PE, anti-IgM-APC and a control fluorescent bait **(A)** or ANDV-specific fluorescent bait **(B)** for 30 min at 4°C. After doublet exclusion (criterion used to discard doublets and capture singlets was forward scatter height versus width and side scatter height versus width), $CD19^{+}/CD27^{+}/IgM^{-}/bait^{+}$ cells were single cell-sorted into a 96-well polymerase chain reaction (PCR) plate using the BD FACSAria II. Data were analyzed using FlowJo v9.x.

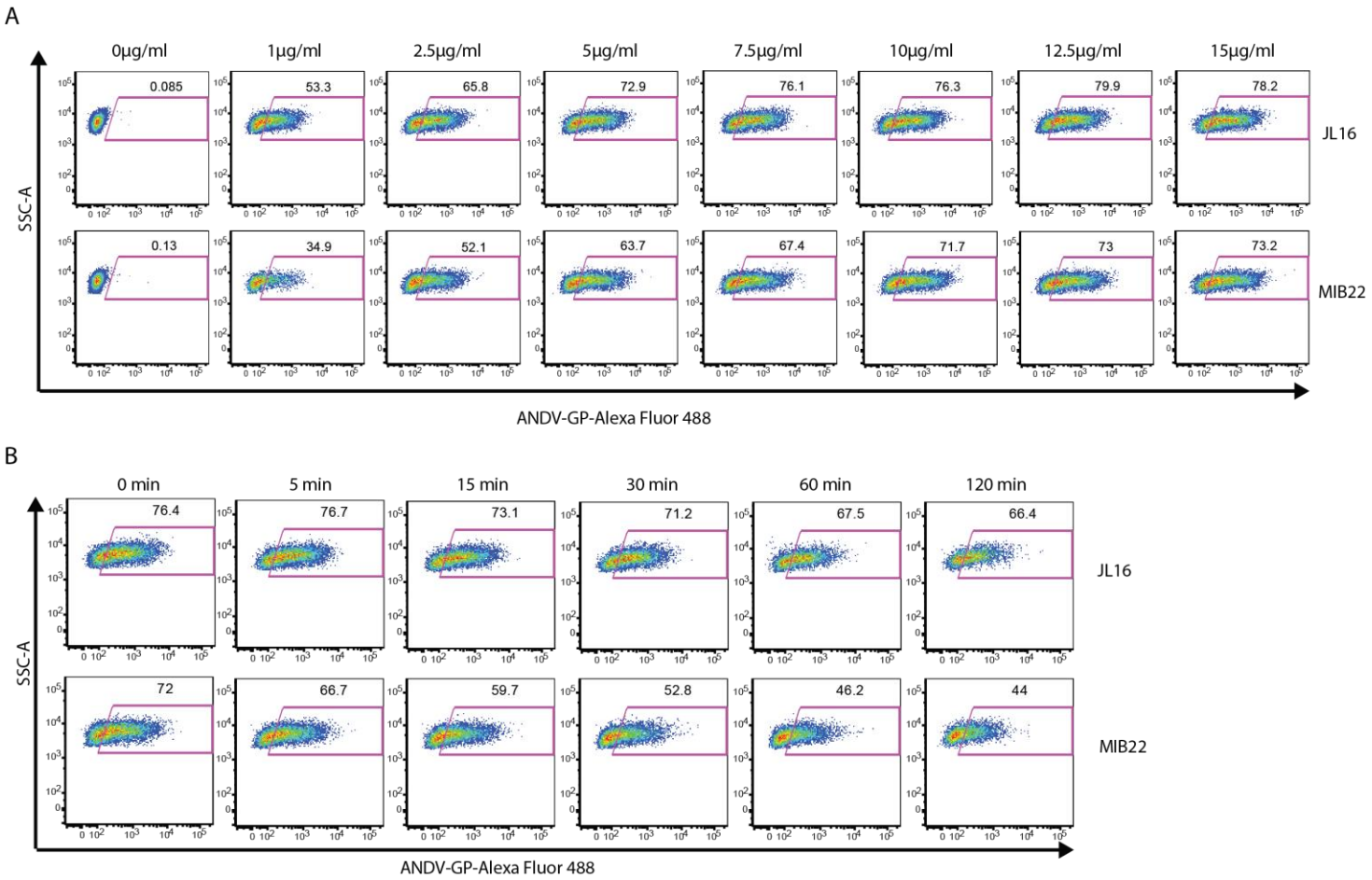

Fig. S3. mAb binding. (A) Representative dot plots of mAb JL16 and MIB22 staining on ANDV-GP-293T cells from 0 to 15µg/ml, binding was detected using a secondary anti-human IgG Alexa Fluor 488 Ab and analyzed by flow cytometry. **(B)** Representative dot plots of mAbs JL16 and MIB22 off-rate determination; binding was determined from time 0 to 120 min.

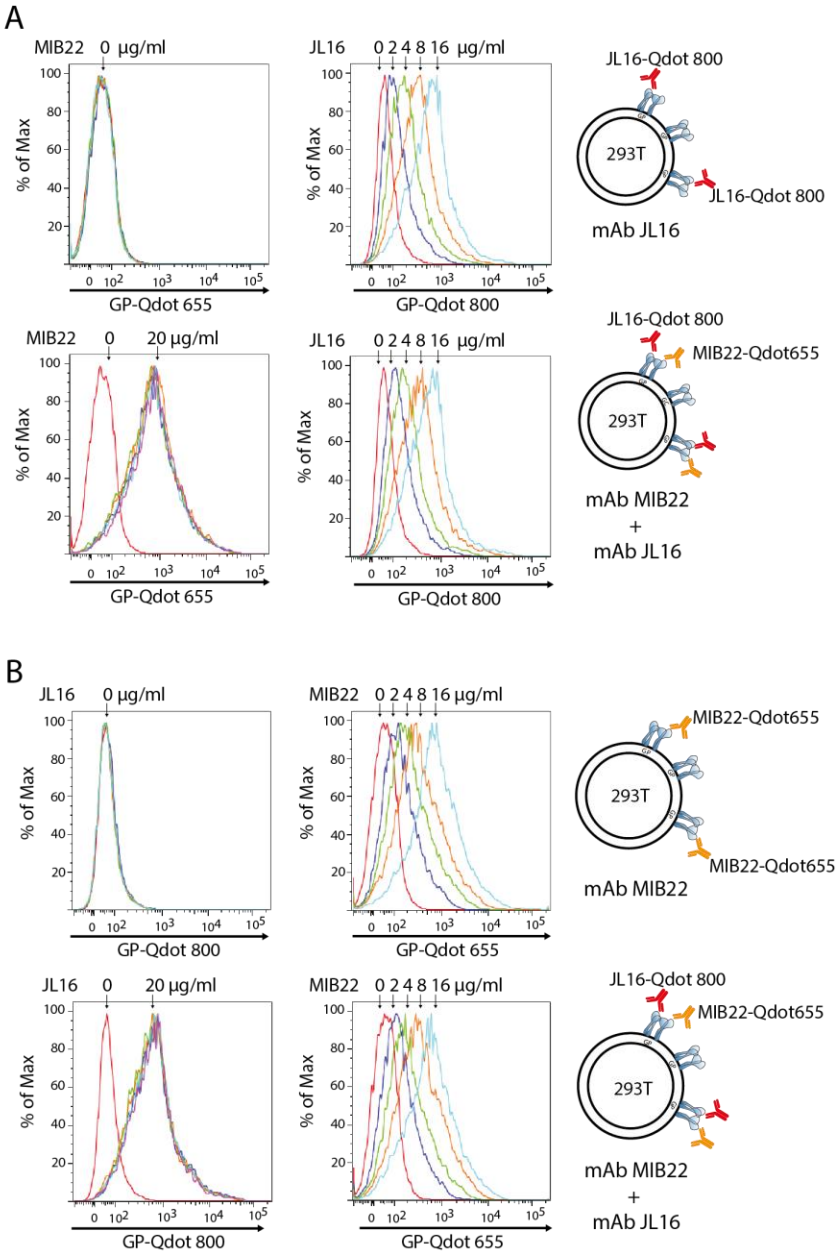
A
MIB22 0 µg/ml
JL16 0 2 4 8 16 µg/ml
% of Max
GP-Qdot 655
GP-Qdot 800
JL16-Qdot 800
293T
mAb JL16
MIB22 0 20 µg/ml
MIB22-Qdot655
mAb MIB22
+
mAb JL16
B
JL16 0 µg/ml
MIB22 0 2 4 8 16 µg/ml
mAb MIB22
JL16 0 20 µg/ml

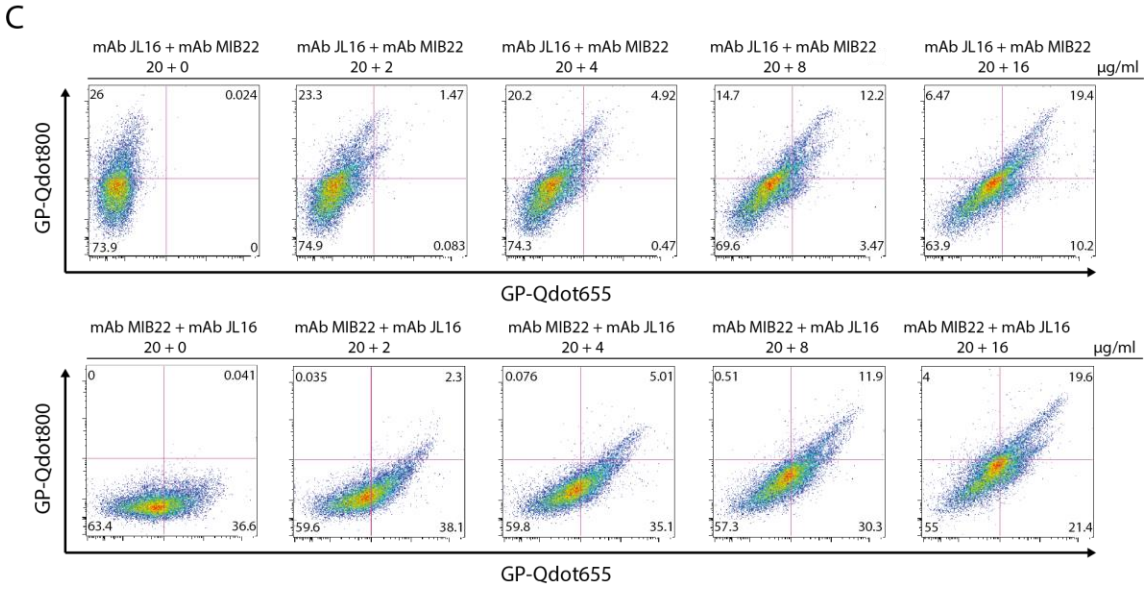
C
mAb JL16 + mAb MIB22
20 + 0
20 + 2
20 + 4
20 + 8
20 + 16
µg/ml
GP-Qdot800
GP-Qdot655
26
0.024
73.9
0
23.3
1.47
74.9
0.083
20.2
4.92
74.3
0.47
14.7
12.2
69.6
3.47
6.47
19.4
63.9
10.2
mAb MIB22 + mAb JL16
0
0.041
63.4
36.6
0.035
2.3
59.6
38.1
0.076
5.01
59.8
35.1
0.51
11.9
57.3
30.3
4
19.6
55
21.4

Fig. S4. Binding competition assay. (A) ANDV-GP-293T cells were stained with JL16-Qdot 800 from 0 to 16 μg/ml (right upper panel). The signal of MIB22-Qdot 655 is shown as a control (left upper panel). For the binding competition assay, ANDV-GP-293T cells were stained with MIB22-Qdot 655 at 20ug/ml and then with JL16-Qdot 800 from 0 to 16 μg/ml (lower panels); representative histograms and a schematic representation of the experiment are shown. **(B)** ANDV-GP-293T cells were stained with MIB22-Qdot 655 from 0 to 16 μg/ml (right upper panel). The signal of JL16-Qdot 800 is shown as a control (left upper panel). For the binding competition assay, ANDV-GP-293T cells were stained with JL16-Qdot 800 at 20 μg/ml and then with MIB22-Qdot 655 from 0 to 16 μg/ml (below graphs), representative histograms and a schematic representation of the experiment are shown. **(C)** Representative dot plots of the competition assay; upper panel shows the staining of ANDV-GP-293T cells with JL16-Qdot 800 at 20 μg/ml and increasing concentrations of MIB22-Qdot 655 (0-16 μg/ml) and the lower panel shows the staining of ANDV-GP-293T cells with MIB22-Qdot 655 and increasing concentrations of JL16-Qdot 800 (0-16 μg/ml).